

# Experimental analysis of atmospheric corrosion of steel S235JR in industrial environment

Jelena N. Stefanović<sup>1</sup>, Zoran Mišković<sup>2</sup>, Stevan Dimitrijević<sup>3</sup>, Zlatko Marković<sup>2</sup> and Milan Spremić<sup>2</sup>

<sup>1</sup>Mining and Metallurgy Institute Bor, Bor, Serbia

<sup>2</sup>The University of Belgrade, Faculty of Civil Engineering, Belgrade, Serbia

<sup>3</sup>Innovation Center of Faculty of Technology and Metallurgy, Belgrade, Serbia

## Abstract

The aim of this study was evaluation of atmospheric corrosion of structural steel S235JR in an industrial environment. General corrosion testing was carried out for six months in the field, at selected atmospheric corrosion stations, near the Sulphuric acid plant, in the Electrolytic refining plant and next to the automatic air quality monitoring station in the city of Bor, Serbia. The results were compared with the standard specimens stored in the laboratory. The steel S235JR specimens were characterized regarding mechanical characteristics by tensile testing. With the aim of assessing the mutual effect of corrosion and polluted industrial environment meteorological parameters were also determined, as well as pollutants in the atmosphere (mainly SO<sub>2</sub>). The X-ray diffraction method was used to identify the composition of corrosion products. Research within this work enabled a better understanding of the behavior of structural steel S235JR in which there was a reduction in load capacity due to corrosion. The corrosion rates obtained under each tested exposure condition showed noticeable differences. It was found that depending on the content of pollutants in the atmosphere and the location of the steel specimen, the corrosion products represented different compounds and solid phases.

**Keywords:** corrosion testing; atmospheric corrosion stations; corrosion products; SO<sub>2</sub>; XRD analysis; standard coupon test

Available on-line at the Journal web address: <http://www.ache.org.rs/HI/>

ORIGINAL SCIENTIFIC PAPER

UDC: 691.714:621.78.019.84

Hem. Ind. 79(1) 19-30 (2025)

## 1. INTRODUCTION

During winter months, the corrosion process proceeds at its fastest rate, due to an increase in the concentration of pollutants in the air, such as sulphur dioxide (SO<sub>2</sub>), carbon dioxide (CO<sub>2</sub>), chloride ions and dust. Industrial environments often involve different mixtures of these elements. Relative humidity, number of hours of sunshine, temperature of air, atmospheric pressure, as well as duration and frequency of rain are among key meteorological variables influencing the corrosion process. The effect of time and quantity of rain are very important for characterizing differences between indoor and outdoor corrosion [1]. Indoor humidity and temperature are largely influenced by the level of ventilation, air conditioning, heating, and thermal isolation [2]. Indoor corrosion intensifies at higher humidity degrees and is affected by the type and level of pollution. Indoor air is polluted from both external and internal sources. Typical indoor pollutants are SO<sub>2</sub>, NO<sub>2</sub>, HCl, H<sub>2</sub>S, organic acids and particles [3]. In general, concentration of particles indoors is the total of those present inside and those brought in from outside.

This study focuses on deterioration of steel elements as a result of corrosion propagation because of the presence of corrosion agents in the industrial environment in the city of Bor, Serbia. Several atmospheric corrosion stations were used for the in-the-field corrosion testing over the period of 6 months. Selected places for corrosion testing were: (1) near the Sulphuric acid plant, close to air quality monitoring station in City park, (2) on the internal balcony above the Electrolysis plant (inside the building) and (3) on the roof of the Mining and Metallurgy Institute Bor, next to the automatic air quality monitoring station.

Corresponding authors: Jelena N. Stefanović, Institut za rudarstvo i metalurgiju Bor, Pariske komune 24, 11070 Novi Beograd

Paper received: 21 November 2024; Paper accepted: 13 March 2025; Paper published: 17 April 2025.

E-mail: [jelena.stankovic@irmbor.co.rs](mailto:jelena.stankovic@irmbor.co.rs)

<https://doi.org/10.2298/HEMIND241121002S>



Steel S235JR was selected for assessment of the corrosion resistance by the analysis of mass loss and evaluation of mechanical properties of specimens after exposure to the tested environments in Bor for a certain period of time. Corrosion products taken from the specimens were subjected to X-ray diffraction (XRD) analysis. XRD analysis is often used in various corrosion studies, such as in improving the control of corrosion processes and preventing the impact of corrosion on water quality degradation in water distribution pipes [4]. Significant differences have been observed in the appearance of corrosion products formed on steel specimens kept in outdoor and indoor conditions.

To obtain a complete characterization of the atmosphere, and thus of the exposure conditions, meteorological data during six months in the period of the experiment duration were analyzed. The indoor conditions of the Electrolysis plant depend on the general environmental conditions of the site. Indoor relative humidity (RH) and temperature depend largely on the degree of ventilation. Pollution by SO<sub>2</sub> alone was considered in this study, being the most common and important corrosive agent. SO<sub>2</sub> indoors is expected to be 30 to 50 % lower than outdoors, as stated in literature [3]. Both mass loss and mechanical properties of the experimental specimens were measured.

Many authors have investigated degradation of mechanical properties of corroded steel. According to recent research, corrosion has reportedly been shown as having no influence on the chemical and mechanical properties of steel [5,6]. However, it clearly affects the reduction of yield plateau, ultimate stress and necking region. It was found that both the bearing capacity and ductile property of structural steel decreased as the corrosion rate increased [7,8].

Corrosion studies that have been carried out in outdoor conditions, were rarely accompanied with those carried out indoors at the same time. The main goal of this work is to provide a deeper insight into how corrosion in outdoor and indoor conditions affects the load-bearing capacity and durability of steel structures, whereby XRD analysis provides additional insight into the process of corrosion. A direct comparison between the corrosion rates of steel in an open atmosphere and in a closed one is presented in this paper.

## 2. EXPERIMENTAL

### 2. 1. Experiment preparation

The standard coupon test specimen was fabricated in accordance with the EN10002-1 standard, the thickness of the coupon for tensile strength testing was 4, 6 and 8 mm. The material used in this experiment was commercial steel S235JR (HBIS Group Serbia Iron & Steel, Serbia). In initial research by the same author [9], steel S235JR was tested on the standard plate 30x40x8 mm, by the use of inductively coupled plasma optical emission spectroscopy (ICP-OES), Ciro Vision (Spectro Analytical Instruments Inc., Germany), with the following chemical composition: 0.12 wt.% C, 0.012 wt.% Si, 0.27 wt.% Mn, 0.012 wt.% Cr, 0.003 wt.% Mo, 0.013 wt.% Ni, 0.005 wt.% P, 0.008 wt.% S, 0.036 wt.% Al, 0.041 wt.% Cu, 0.0003 wt.% B, 0.0006 wt.% Sn, 99.40 wt.% Fe and others in a small percentage.

### 2. 2. Atmospheric corrosion stations

Tests for corrosion resistance were conducted at atmospheric corrosion stations, under actual operating circumstances. These were carefully chosen locations within the industrial complex, where specimens are displayed, and corrosion-related changes are tracked.

In this study, atmospheric corrosion stations are selected for accelerated testing of Bor industrial zone. The industrial zone in Bor is in the very center of the city, so the Sulfuric acid plant is located near center of the town. The atmospheric corrosion stations were chosen next to air quality monitoring stations, in the City park and at the Mining and Metallurgy Institute Bor. The distance between these two locations is about 3 km. The automatic monitoring station in the City park is about 800 m away from the Sulfuric acid plant. This part of the study has been carried out in outdoor conditions. Another location was inside the Electrolytic refining plant (Figure 1). Steel specimens were exposed for 6 months in winter between November 2016 and May 2017. There were 6 specimens at each location, a total of 18, placed on a wooden frame, at an angle of 45° to the ground, horizontally, and facing south. It is frequently considered as the position where the specimen's greatest surface gets corroded [10,11]. In this research, there was an attempt to obtain the degradation of the material due to corrosion under real industrial conditions, in the winter months.



Figure 1. Location of the stations across the industrial area of Bor: (1) near the Sulphuric acid plant; (2) inside the Electrolytic refining plant; (3) next to the automatic air quality monitoring station in the Mining and Metallurgy Institute Bor

After exposure, corrosion products from all specimens, as well as from the reference specimen, were removed according to ISO 8407:2021 [12]. This standard specifies procedures for removal of corrosion products from metals and alloys, which are created on specimens for corrosion testing during their exposure to the corrosive media. On the test specimens, the products were first removed mechanically, and then chemically, for the duration defined in the standard. The procedures set out in this standard are intended to remove corrosion products without significant removal of the parent metal. To determine the mass loss of parent metal when removing the corrosion product, the parallel uncorroded, reference specimen is cleaned by the same procedure as the specimen under test. After removing the corrosion products, all specimens, 18 of them, were subjected to a standard coupon test.

### 2. 3. Standard coupon test

Standard coupon tests were conducted in this study to assess the mechanical properties, strength and the module of elasticity of specimens under different corrosion conditions. Standard coupon tests were carried out on a servo-hydraulic universal testing machine (Instron 1332 with Fast Track 8800 control system, Instron, USA) at a maximum load of 100 kN and an extensometer with a gauge length of 50 mm was installed in the middle of the specimen to measure the deformation during the standard coupon test.

### 2. 4. XRD analysis

XRD analysis was conducted to identify corrosion products formed at the three different exposure sites (Figure 1):

1. near the Sulphuric acid plant (AF)
2. inside the Electrolytic refining plant (EF)
3. next to the automatic air quality monitoring station in the Mining and Metallurgy Institute Bor (MP)

The X-ray diffraction was performed using a RIGAKU Ultima IV (Tokyo, Japan) diffractometer with Ni-filtered Cu K $\alpha$  radiation ( $\lambda = 0.1540$  nm), with the X-ray tube operating at 40 kV and 40 mA. The XRD patterns of the corrosion products were recorded over the 5– 90°  $2\theta$  range with a step of 0.02° and a scanning rate of 10° min<sup>-1</sup>. The phase analysis was conducted using the PDXL2 software (version 2.0.3.0) [13].

### 2. 5. Meteorological parameters and atmospheric pollutants

Some of the most important meteorological parameters in Bor for the corrosion process are shown in Table 1.

Table 1. Monthly average meteorological parameters (*T* is temperature, *RH* is relative humidity and *TOW* is the time of wetness) [14]

Measurement period	<i>T</i> / °C	<i>RH</i> , %	<i>TOW</i> , h	Rainfall, mm m <sup>-2</sup>	Atmospheric pressure, kPa*
November 8 <sup>th</sup> 2016 - December 8 <sup>th</sup> 2016	6.9	70	168	50.0	97.63
December 9 <sup>th</sup> 2016 - January 8 <sup>th</sup> 2017	2.5	69	192	7.4	98.41
January 9 <sup>th</sup> 2017 - February 8 <sup>th</sup> 2017	0.4	83	144	47.0	97.05
February 9 <sup>th</sup> 2017 - March 8 <sup>th</sup> 2017	6.7	79	360	24.7	97.01
March 9 <sup>th</sup> 2017 - April 8 <sup>th</sup> 2017	6.6	79	240	21.1	96.75
April 9 <sup>th</sup> 2017 - May 8 <sup>th</sup> 2017	12.4	72	120	42.7	96.81

Time of wetness (TOW) was estimated from the number of hours per year that the relative humidity was equal to or above 85 % and the temperature exceeded 0 °C.

Average of SO<sub>2</sub> values in Table 2 are reported in the Annual report on air quality in the Republic of Serbia, Ministry of Environmental Protection, Environmental protection agency [15,16]. As can be seen, differences in SO<sub>2</sub> concentration are noticeable between these two stations.

Table 2. Monthly average SO<sub>2</sub> deposition [15, 16]

Measurement period	SO <sub>2</sub> deposition, mg m <sup>-2</sup>	
	Air quality MP monitoring station	Air quality monitoring station in City park
November 8 <sup>th</sup> 2016 - December 8 <sup>th</sup> 2016	26.4	26.2
December 9 <sup>th</sup> 2016 - January 8 <sup>th</sup> 2017	29.0	26.0
January 9 <sup>th</sup> 2017 - February 8 <sup>th</sup> 2017	54.1	66.8
February 9 <sup>th</sup> 2017 - March 8 <sup>th</sup> 2017	24.7	59.3
March 9 <sup>th</sup> 2017 - April 8 <sup>th</sup> 2017	20.4	43.6
April 9 <sup>th</sup> 2017 - May 8 <sup>th</sup> 2017	16.0	42.3
Calculated average value	28.4	44.0
The maximum measured value	272.6 (measured on 01. 02. 2017)	299.9 (measured on 01.05.2017)

Environmental parameters that influence atmospheric corrosion, such as relative humidity, temperature and deposition rates, vary significantly between indoor and outdoor conditions.

The indoor conditions in the Electrolytic refining plant are near constant in terms of temperature, relative humidity and the concentration of pollutants in the air. Blowers were installed inside the Electrolysis plant, which permanently ventilated the facility. The temperature inside the plant ranged between 13 and 18 °C in the relevant period. The atmosphere also contained electrolyte aerosols. The electrolyte had the following composition: H<sub>2</sub>SO<sub>4</sub> 1.7 mol dm<sup>-3</sup>, CuSO<sub>4</sub>·5H<sub>2</sub>O ≈ 160 g l<sup>-1</sup>, or about 40 g l<sup>-1</sup> of copper, and HCl 0.04 mol dm<sup>-3</sup>. The higher humidity indoors, which was always higher than 80 %, was mainly influenced by the open electrolytic cells and a high electrolyte temperature (58 ± 2 °C).

### 3. RESULTS AND DISCUSSION

#### 3. 1. X-ray diffraction analysis

The X-ray diffraction was performed on corrosion products removed from the specimens, one from each of the three locations. Main corrosion products of carbon steels are reported to be lepidocrocite (γ-FeOOH) and goethite (α-FeOOH) regardless of atmospheric conditions, even the industrial [17,18]. During the time of exposure, lepidocrocite is transformed to goethite, and SO<sub>2</sub> highly influences this process [19], which proceeds in several parallel and consecutive stages [20]. In these corrosion processes, magnetite (Fe<sub>3</sub>O<sub>4</sub>) and maghemite (γ-Fe<sub>2</sub>O<sub>3</sub>) are practically intermediates and are often detected by the XRD analysis. However, these minerals are hard to differentiate as a consequence of their almost identical crystalline structure [21]. They are usually close to the surface of the steel, leading to their identification but without determination of their quantity portion in the corrosion products. A percentage of the total identified crystalline products is given from a semi-quantitative estimate for each detected phase, where it could be expressed quantitatively.

The corrosion products of the first sample AF contain 57 wt.% lepidocrocite (γ-FeOOH) and 43 wt.% goethite (α-FeOOH) (Figure 2). The second sample EF contains 33 wt.% goethite (α-FeOOH), 20 wt.% rozenite (FeSO<sub>4</sub>(H<sub>2</sub>O)<sub>4</sub>) and 47 wt.% jarosite (KFe<sub>3</sub>(SO<sub>4</sub>)<sub>2</sub>(OH)<sub>6</sub>) (Figure 3). The third sample MP contains 68 wt.% lepidocrocite (γ-FeOOH) and 32 wt.% goethite (α-FeOOH) (Figure 4). Magnetite (Fe<sub>3</sub>O<sub>4</sub>) and maghemite (γ-Fe<sub>2</sub>O<sub>3</sub>) are not quantified but detected in all three samples. Lepidocrocite was also identified in the EF specimen, although not quantified.

Figure 2 presents the XRD pattern for the sample AF exposed to industrial atmospheric conditions with a high SO<sub>2</sub> concentration (sulphuric acid plant). The diffractogram shows peaks of γ-FeOOH at the 2θ angles of 14.10, 27.04, 36.48, 46.88, 52.98 and 60.98°; additionally, peak at 84.70° can also be attributed to the same compound. Moreover, the relative intensity of these peaks has the same pattern as the single high-purity crystal phase, further confirming its dominant presence. It is the primary component of the surface corrosion layer, with a content of 57 vs. 43 wt.% of α-FeOOH.

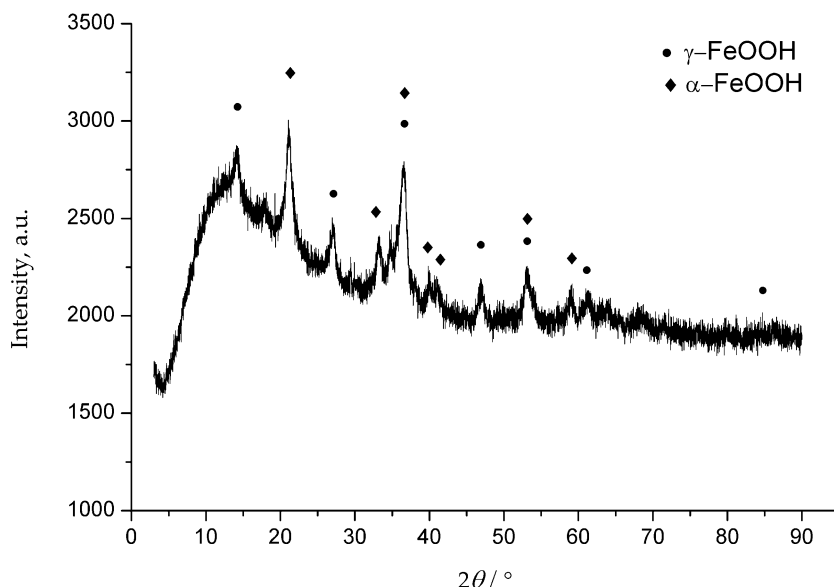


Figure 2. X-ray diffractogram of corrosion products of steel S235JR after 6 months of exposure near the Sulphuric acid plant in Bor (AF)

The ratio between these two variants of FeOOH is less favourable for the  $\gamma$  type of this iron oxyhydroxide in industrial atmosphere (at AF), than for a nonindustrial atmosphere (at MP) as a corrosion environment (Figure 4). This was expected due to the presence of higher  $\text{SO}_2$  concentrations in the air (Table 2) that influence the transformation of lepidocrocite into goethite, since  $\text{SO}_2$  dissolves the initially formed  $\gamma$ -FeOOH, promoting this phase transformation, as explained in other study [22]. In the diffractogram the presence of the peaks of  $\alpha$ -FeOOH are also unquestionable and clear as well. These peaks are at the following positions 21.12, 33.18, 36.60, 39.86, 40.94, 53.12 and 59.16°. The presence of maghemite, peaks at 35.52° (overlapped with all other detected crystal phases), 53.46, 57.30 and 62.86°, and magnetite with peaks at 18.22 29.96 and 35.34° (overlapped with all other detected crystal phases), 62.56° have also been confirmed by XRD analysis. However, these minerals were in low quantities, practically as trace compounds.

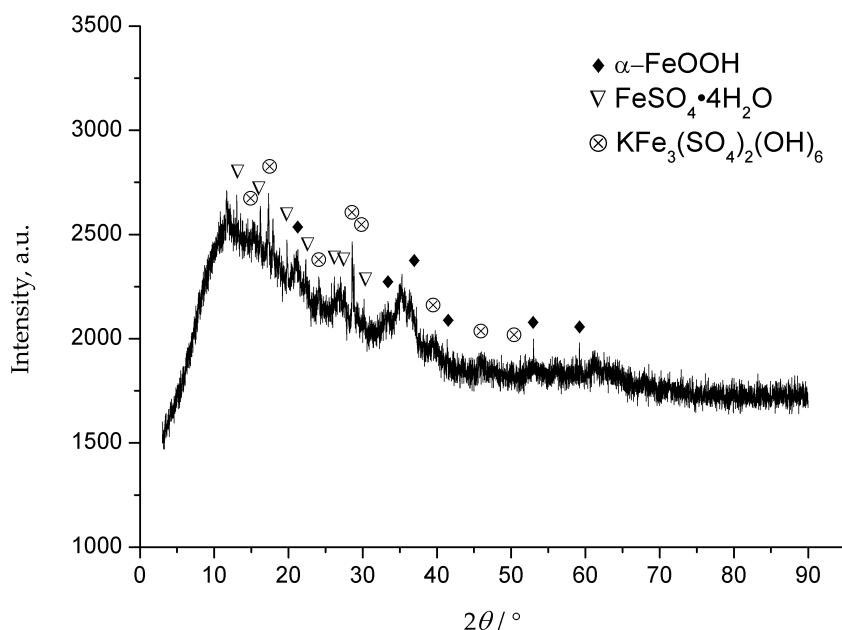
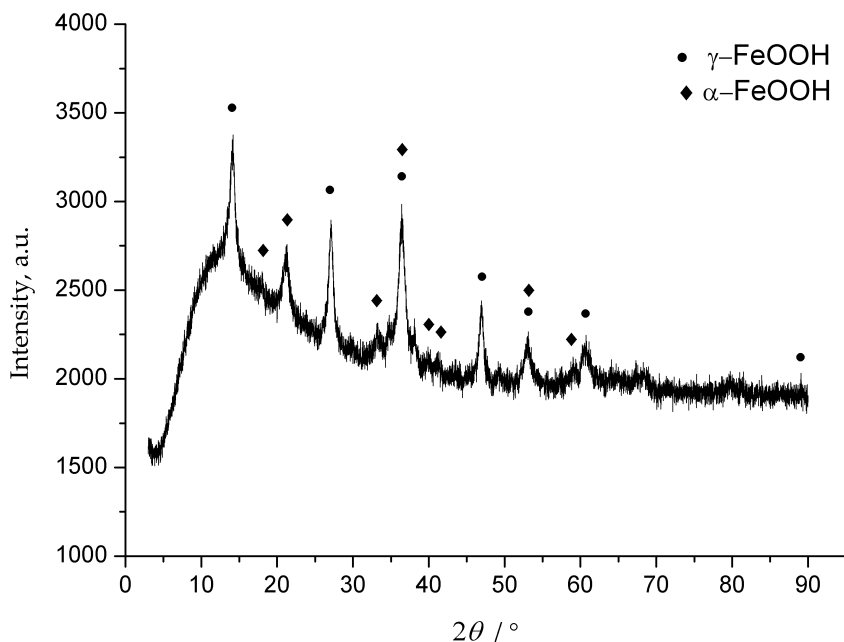


Figure 3. X-ray diffractogram of corrosion products of steel S235JR after 6 months of exposure into the

*Electrolytic refining plant in Bor (EF)*

*Figure 4. X-ray diffractogram and corrosion products of steel S235JR after 6 months of exposure next to the automatic air quality monitoring station in Mining and Metallurgy Institute Bor (MP)*

Figure 4 shows the results of the XRD analysis of the steel exposed to relatively mild atmospheric conditions at MP in a six-month period. Corrosivity category for this atmosphere conditions is C2-C3 according to ISO 9223:2012 [23]. The XRD diffractograms in Figures 2 and 4 are relatively similar.. Two main constituents are gamma and alpha FeOOH. The first has diffraction peaks at 14.08, 27.08, 36.36, 46.90, 52.96, 60.74 and 89.06° which is almost identical to the appearance in Figure 2 with the better (closer to the reference) position of the peak at the highest  $2\theta$  angle. Here, it should be noted that even a peak with a low intensity, at 18.0°, was detected. These more complete XRD patterns of these phases indicate even lower content of other crystal phases (maghemite and magnetite) and amorphous forms of the corrosion products compared to the influence of the industrial environment. The magnetite neither showed the peak at  $2\theta$  angle of 18°, nor it was overlapped with the  $\alpha$ -FeOOH. Nevertheless, maghemite peak at 30.16° was observed in the diagram. It has to be stressed that the semi-quantitative XRD determination of the relative contents is in accordance with the values of the peak intensities of  $\gamma$ -FeOOH when compared the Figures 2 and 4. Higher intensity of the main component of the corrosion layer corresponds to the higher relative content, as also reported by other authors [22].

The diffractogram in Figure 3 is the most complex of those three and much different from the other two. The main differences are a low content of  $\gamma$ -FeOOH and the presence of rozenite ( $\text{FeSO}_4(\text{H}_2\text{O})_4$ ) and jarosite ( $\text{KFe}_3(\text{SO}_4)_2(\text{OH})_6$ ) at the steel surface exposed in the specific industrial atmosphere at EF. The fumes of sulfuric acid and copper sulfate conditioned the appearance of these corrosion products. This presents a clear explanation for the appearance of rozenite, although additional considerations are needed to explain the presence of jarosite. The occurrence of jarosite as a product of atmospheric corrosion is not typical but was observed in marine atmospheric environments at the similar steel type (S235JR), where chloride ions with the presence of sulfate ions lead to precipitation of jarosite phase together with potassium, which originated mainly from the emissions from the oil-fired power plant and less from the marine aerosols [17]. Here, the proximity of the power plant operation and a flash smelter powered by oil in the period of exposure certainly had an influence. However, authors consider that potassium presence was primarily from the additives used in EF, being also constituents of aerosols.

The full pattern of  $\alpha$ -FeOOH: 21.12, 33.22, 36.54, 41.36, 53.04 and 59.22° ( $2\theta$  angles) is present in Figure 3 and it is a second crystal phase by amount. Rozenite ( $\text{FeSO}_4 \times 4\text{H}_2\text{O}$ ) is a new crystal component characterized by the

following peaks 13.02, 16.16, 19.80, 22.26, 26.18, 27.68 and 30.18°. It comprises about a fifth of the total corrosion products. Jarosite was the most abundant component of the corrosion layer (47 wt.% of the total quantity). All main peaks of this phase were present in the diffractogram: 15.02, 17.34, 24.32, 28.60, 28.82, 39.32, 45.96 and 49.98°. Although the presence of this crystal component is semi-quantitatively determined, its very high content was not expected and needs more research to be fully explained.  $\gamma$ -FeOOH was identified but only by the three peaks at 27.02, 36.34 and 61.04°, indicating the low content. Magnetite and maghemite also did not show a full XRD pattern in the diagram as well, and identification of these minerals was further complicated by some of the peaks being overlapped. Although not identified by the software, presence of magnetite ( $\text{Fe}_3\text{O}_4$ ) in traces was possible, with pointed out peaks at 33.00 and 35.62° and partly at 49.54 and 54.16°. However, the other characteristic peaks were not visible in the XRD spectrum. Figure 3 shows also a few unmarked peaks that could indicate melanterite ( $\text{FeSO}_4 \cdot 7\text{H}_2\text{O}$ ) and siderotil ( $\text{FeSO}_4 \cdot 5\text{H}_2\text{O}$ ), but the presence of these minerals is not definite, although probable due to the sulphate presence.

Figures 2 to 4 show XRD patterns of corrosion products at the steel surface influenced by atmospheric conditions at three different locations. The X-ray diffraction patterns had a very similar look independent of the exposure conditions, except for the diffraction pattern of the specimen in the EF. The crystalline products formed in the rust layer are lepidocrocite ( $\gamma$ -FeOOH) and goethite ( $\alpha$ -FeOOH), which are typical in the case of atmospheric corrosion of carbon steel, as it is found also in other studies [19,20]. The common feature is a very pronounced noise throughout the whole XRD diffractogram due to a high number (and amount) of amorphous components without a well-defined Bragg peak [18]. Additionally, it is influenced by crystal forms of compounds present at relatively low contents (under 5 wt.%).

### 3. 2. Corrosion rate

The mass loss for each group of the specimens with the same thickness after the exposure to different atmospheric conditions was calculated by:

$$\Delta m = m_0 - m - \frac{\sum_{i=1}^2 (m_{0,i} - m_i)}{2} \quad (1)$$

where  $\Delta m$  is the mass loss due to corrosion,  $m_0$  is the initial mass prior to the corrosion test,  $m$  is the mass after the corrosion test,  $m_{0,i}$  and  $m_i$  are the mass of control specimens before and after chemically cleaning, respectively. After the determination of the initial total surface area of specimen A and the mass loss during the test  $\Delta m$ , the average corrosion rate in the first year was obtained in accordance with ISO 9226:2012 [24]. The corrosion rates of S235JR steel are expressed as a mass loss per unit area over time ( $r_{\text{corr}}$ ) or as a thickness reduction over time ( $r_{\text{corr}}'$ ), given in Table 3.

Table 3. Corrosion rate values and mass loss of steel specimens of different nominal thicknesses after 6 month exposure

Location	Nominal thickness, mm (2 specimens)	Initial mass, g	Mass loss, g	$r_{\text{corr}} / \text{g m}^{-2} \text{ year}^{-1}$	$r_{\text{corr}}' / \mu\text{m year}^{-1}$
1. Sulphuric acid plant, AF (outdoor)	4	253.66±1.05	6.41±0.02	68.39±0.28	8.71±0.04
	6	385.07±2.92	7.28±0.10	72.53±1.03	9.23±0.13
	8	520.14±1.57	7.64±0.16	71.33±1.45	9.07±0.18
2. Electrolytic refining plant, EF (indoor)	4	253.76±0.69	0.82±0.01	8.73±0.12	1.11±0.01
	6	384.87±0.85	0.98±0.01	9.78±0.12	1.25±0.02
	8	512.52±12.36	0.97±0.11	8.98±1.00	1.14±0.13
3. The automatic air quality monitoring station in MMI Bor, MP (outdoor)	4	254.95±2.09	2.03±0.04	21.60±0.41	2.75±0.06
	6	384.54±0.78	2.29±0.01	22.83±0.19	2.91±0.02
	8	517.15±5.74	1.95±0.52	18.15±4.86	2.31±0.62

The results of this study provide a direct comparison between the corrosion rates of steel specimens placed in outdoor and indoor conditions. In general, the indoor corrosion rates are relatively low (Table 3) due to the absence of precipitation and fog as well as higher indoor temperatures (often above the dew point), which significantly reduce the wetness duration. The outdoor corrosion rate is always higher than the indoor one, independent of the specimen thickness. Steel specimens placed outdoors are exposed to day/night change and occasionally to dew, rain, and/or fog.

At the same time, pollutant deposition is higher than that in indoor conditions. Corrosion products formed outdoor undergo significant changes as they frequently dry out during the day and absorb humidity at night, occasionally becoming wet due to rain, dew or fog.

### 3. 3. Mass and load bearing loss

Table 4 shows the reference values for etalon specimens, mass loss due to chemical cleaning and the maximum force shown here for comparison with values of specimens determined after corrosion presented in Table 5. The maximum force denotes the peak load recorded on the force-elongation curve and is used to calculate the ultimate tensile stress based on the specimen's initial cross-sectional area. To quantify the influence of corrosion, mass loss, maximum force after corrosion and depth are also shown in Table 5. Results indicated that with an increment in corrosion, mass, depth and maximum force significantly decreased. In Table 5, the change in depth  $\Delta d_{\text{mass}}$  based on mass loss is also shown, representing the difference between the depth before corrosion and after corrosion. Depth before corrosion and after corrosion based on mass loss are determined as follows:

$$d_0 = \frac{m_0}{A_w D} \quad (2)$$

$$d_1 = \frac{m_1}{A_w D} \quad (3)$$

where  $m_0$  and  $m_1$  are mass before and after expose to corrosion, respectively,  $A_w$  is the surface area of the specimen, and  $D$  is the density.

Table 4. Etalon specimens before and after chemically cleaning

Nominal thickness, mm (2 specimens)	$m_0$ / g	$d_0$ / mm	$m_1$ / g	$d_1$ / mm	$F_{\text{max}}$ / N
4	252.55±2.98	4.01±0.05	252.48±2.95	4.01±0.05	31624±755
6	386.74±1.22	6.14±0.02	386.70±1.22	6.14±0.02	50835±1261
8	517.28±5.92	8.21±0.09	517.25±5.93	8.21±0.09	62858±1044

Each values in the tables 3, 4 and 5 is expressed as the mean ± standard deviation calculated from two individual measurements. Preliminary results related to the 8 mm specimens were reported in previous publications [9]. This paper presents the comprehensive findings for all three specimens thicknesses.

Table 5. Specimens before and after exposure to corrosion

Location	Nominal thickness, mm (2 specimens)	$d_0$ / mm	$d_1$ / mm	Mass loss, %	$\Delta d_{\text{mass}}$ / mm	$F_{\text{max}}$ / N
1. Sulphuric acid plant, AF	4	4.03±0.02	3.93±0.02	2.53±0.00	0.10±0.00	30146±205
	6	6.12±0.05	6.00±0.05	1.89±0.04	0.12±0.00	49152±1613
	8	8.26±0.02	8.14±0.03	1.47±0.03	0.12±0.00	61826±206
2. Electrolytic refining plant, EF	4	4.03±0.01	4.02±0.01	0.32±0.00	0.01±0.00	31273±358
	6	6.11±0.01	6.10±0.01	0.25±0.00	0.02±0.00	50067±658
	8	8.14±0.20	8.12±0.20	0.19±0.03	0.02±0.00	62268±1253
3. The automatic air quality monitoring station in Mining and Metallurgy Institute Bor, MP	4	4.05±0.03	4.02±0.03	0.79±0.01	0.03±0.00	30982±257
	6	6.11±0.01	6.07±0.01	0.60±0.01	0.04±0.00	51248±1519
	8	8.21±0.09	8.18±0.08	0.38±0.10	0.03±0.01	62715±832

After the coupon tests, the load and displacement results of the S235JR specimens exposed to different corrosion conditions were obtained. Figure 5 shows force-elongation curves of corroded and uncorroded test steel S235JR specimens of different nominal thickness. The main reason for the decrease in the maximum force is the effective reduction of the cross-sectional area of the corroded specimen. It is worth noting that the force decrease was greater in the case of a higher corrosion rate.

In the industrial atmosphere of Bor, near to AF, the colour of the rust from steel specimens is in dark brown tones; granulations of corrosion layers are larger, while on the specimens in the EF and MP granulation of corrosion layers is

smaller, similar to ground powder. The dark brown colouring of the rust is the result of the presence of SO<sub>2</sub> at high concentrations and accelerating transformation of lepidocrocite into goethite [25]. In accordance with the statements of other authors [1], transformation of lepidocrocite to goethite is a measure of the corrosion process extension, so that this complies with the fact that lower corrosion is obtained at MP than near to AF in Bor. Corrosion products were definitely more compact and less porous when they are exposed to indoor conditions than outdoor conditions (they have a better protective function, which was also observed during the removal of corrosion products when measuring the mass loss). The compact corrosion products are the reason for lower mass loss (slower general corrosion) of these specimens. On the other hand, corrosion products formed outdoors exhibit layered deposits and cracks.

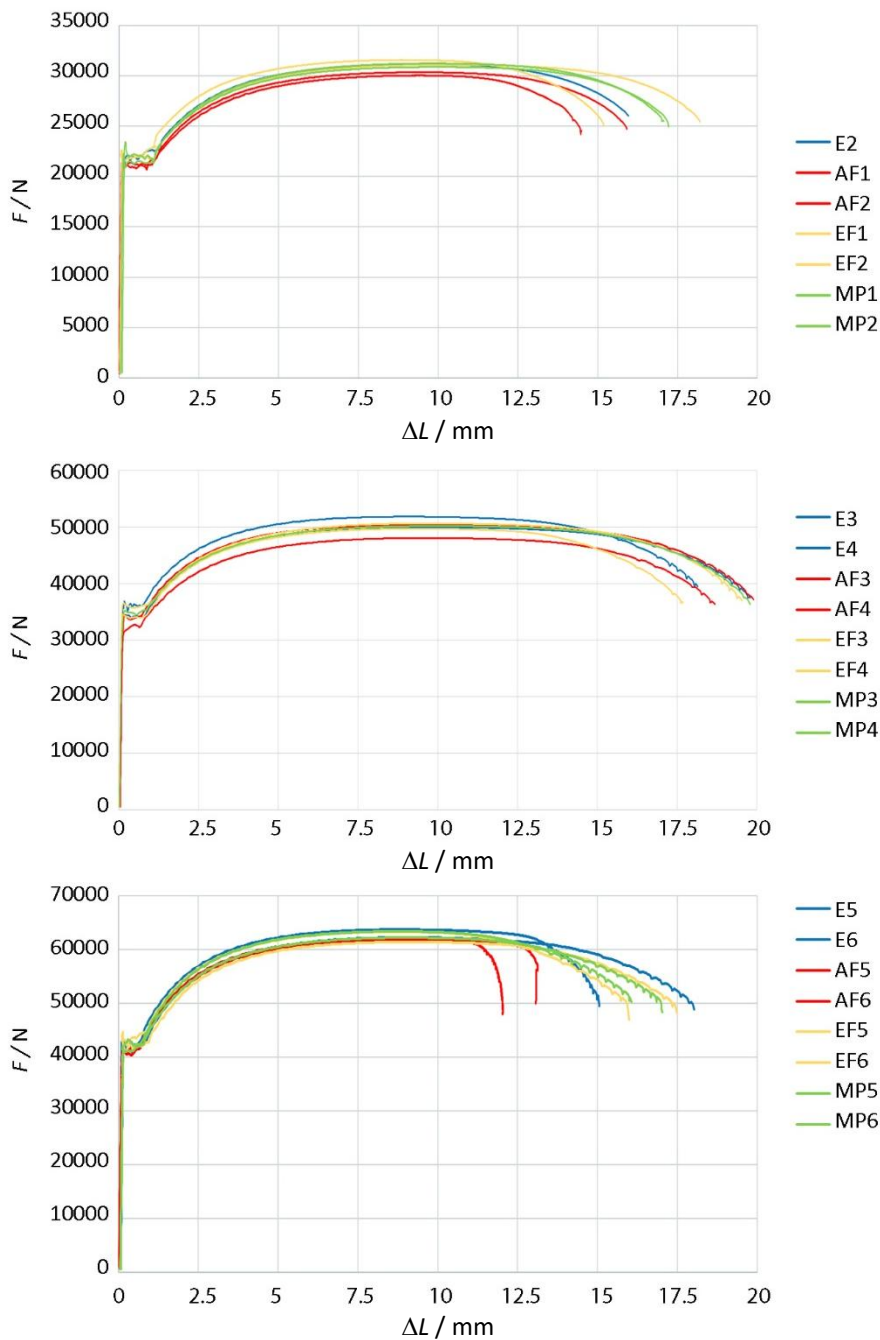


Figure 5. Load-displacement relationships for etalon specimens (E) and tested specimens at AF, EF and MP for specimen thicknesses of: A) 4 mm (specimens are labeled with 1 and 2); B) 6 mm (specimens are labeled with 3 and 4); C) 8 mm (specimens are labeled with 5 and 6)



Atmospheric corrosion is quantitatively assessed by measuring the mass loss and then determining the corrosion rate for each location separately. A higher corrosion rate is always obtained for specimens closer to the AF. Specimens that were exposed to corrosive agents from the outside, near the AF and next to MP, were uniformly corroded, while the dominant pitting corrosion can be observed in the specimens in EF. The highest corrosion rate values are generally associated with higher SO<sub>2</sub> levels in the air. For the corroded steel specimens, the reduction of maximum force is not linearly proportional to the degree of mass loss (Table 5). The cause of this finding is the appearance of pitting corrosion along with uniform corrosion, as well as the influence of local effects due to the inequalities on the specimens found after exposure to corrosion. Local pitting corrosion has a significant impact on strength reduction in addition to the section loss. It leads to fracture where the test specimens are weakest. The change in the path of fracture, with the development of corrosion, is also related to pitting corrosion.

In Figure 5, specimens from the same location are marked with the same colour. The force-elongation curves of the corroded specimens constantly decreased as the corrosion rate increased. Less corroded specimens (MP) have a larger "necking" area, while in more corroded specimens (AF), the "necking" area decreases together with the ductility of the elements. Specimens that suffered a greater mass loss (AF), become less ductile, due to local material damage that cannot be described by a uniform corrosion rate law and a uniform surface degradation. This statement is in agreement with the observations in a previous experiment [26] showing that in extreme corrosion cases, the yield plateau of the stress-strain curves of the corroded specimens shrinks and, in certain cases, completely vanishes, signifying a change in the steel elements, from ductile to brittle fracture.

#### 4. CONCLUSION

Interaction between corrosion of steel elements and pollutants in the atmosphere is of great importance for corrosion research. The consequence of this interaction is degradation and destruction of steel structures. Corrosion of steel in an industrial environment can be uniform, developing equally over the entire surface of the metal which is characteristic of outdoor conditions, or localized, pitting corrosion (present in indoor conditions in the present study).

Uniform corrosion occurs through uniform corrosion layers of similar composition, while pitting corrosion creates types of corrosion products that differ in composition and proportions of their components, which is determined by XRD analysis in this paper. This primarily refers to the specimens that were in the indoor of the Electrolytic refining plant and for which the corrosion products were much more complex in composition than the products formed at the outdoor stations. It can be concluded that steel specimens exposed to indoor conditions experience less severe conditions, but also additional type of corrosion (pitting).

XRD analysis was used in this study as a relationship indicator between the composition of corrosion products and the type of environment in which corrosion develops. The results and data obtained in this work should contribute to the understanding of the problem of strength capacity and durability of steel structures weakened by corrosion in industrial environments such as in Bor.

**Acknowledgements:** This work was financially supported by the Ministry of Science, Technological Development and Innovation of the Republic of Serbia, as well as the Contract on realization and financing of the scientific research work of the Mining and Metallurgy Institute Bor in 2024, contract number: 451-03-66/2024-03/200052 and also No. 200092, Faculty of Civil Engineering, University of Belgrade and 451-03-66/2024-03/200287, IC TMF. We are also kindly thankful to the Mining and Metallurgy Institute Bor for funding part of the laboratory work. The authors wish to thank Silvana Dimitrijević for help within the laboratory experiment and Zoran Avramović for field work.

#### REFERENCES

- [1] Mendoza A, Corvo F. Outdoor and indoor atmospheric corrosion of carbon steel. *Corros Sci.* 1999; 41: 75-86. [https://doi.org/10.1016/S0010-938X\(98\)00081-X](https://doi.org/10.1016/S0010-938X(98)00081-X)
- [2] Gil H, Calderón J. A, Buitrago C. P, Echavarría A, Echeverría F. Indoor atmospheric corrosion of electronic materials in tropical-mountain environments. *Corros Sci.* 2010; 52(2): 327-337. <https://doi.org/10.1016/j.corsci.2009.09.019>

- [3] Del Angel-Meraz E, Corvo F, Hernandez-Morales N, Tejero-Rivas M. Particularities of indoor atmospheric corrosion of steel inside electric boxes in the tropical climate of Tabasco, Mexico. *Indoor Built Environ.* 2020; 30(10): 1609-1619. <https://doi.org/10.1177/1420326X20950411>
- [4] Rajaković-Ognjanović V, Grgur B. Corroded scale analysis from water distribution pipes. *Hem. Ind.* 2011; 65(5): 507-515. <https://doi.org/10.2298/HEMIND110523049R>
- [5] Xue X, Hua J, Wang F, Wang N, Li S. Mechanical Property Model of Q620 High-Strength Steel with Corrosion Effects. *Buildings.* 2022; 12: 1651. <https://doi.org/10.3390/buildings12101651>
- [6] Zhao N, Zhang C. Experimental Investigation of the Mechanical Behavior of Corroded Q345 and Q420 Structural Steels. *Buildings.* 2023; 13: 475. <https://doi.org/10.3390/buildings13020475>
- [7] Di Sarno L, Majidian A, Karagiannakis G. The Effect of Atmospheric Corrosion on Steel Structures: A State-of-the-Art and Case-Study. *Buildings.* 2021; 11: 571. <https://doi.org/10.3390/buildings11120571>
- [8] Li F, Cui C, Ma R, Tian H. An experimental study on the corrosion behaviors and mechanical properties of Q345qD steel in neutral salt spray environment considering stress state. *Dev Built Environ.* 2023; 15: 100214. <https://doi.org/10.1016/j.dibe.2023.100214>
- [9] Stefanović J, Dimitrijević S, Filipović S, Đorđević J. Evaluation of the corrosion resistance of steel elements in the industrially aggressive environments using the accelerated corrosion testing methods. *Min Metall Eng Bor.* 2023; 1: 53-60. <https://doi.org/10.5937/mmeb2104053S>
- [10] Sanders C, Santucci R. Jr. Experimental Design Considerations for Assessing Atmospheric Corrosion in a Marine Environment: Surrogate C1010 Steel. *Corros Mater Degrad.* 2023; 4(1): 1-17. <https://doi.org/10.3390/cmd4010001>
- [11] Parekh SP, Pandya AV, Kadiya HK. Progressive Atmospheric Corrosion Study of Metals Like Mild Steel, Zinc and Aluminum in Urban Station of Ahmedabad District. *Int J Chemtech Res.* 2012; 4: 1700-1774. <http://dx.doi.org/10.1155/2009/807376>
- [12] ISO Standard 8407:2021 Corrosion of Metals and Alloys: Corrosivity of atmospheres: Removal of Corrosion Products from Corrosion Test Specimens. <https://www.iso.org/standard/71866.html>
- [13] PDXL, Version 2.0. 3.0 Integrated X-ray Powder Diffraction Software, Rigaku Corporation. Tokyo, Japan; <https://rigaku-pdxl.software.informer.com/2.0/>
- [14] Annual and monthly reports on ambient air quality in Bor for the period 2016-2017 (Archive MMI Bor), Mining and Metallurgy Institute Bor (MMI Bor), Laboratory for Chemical Testing, Department for Environmental Protection and Climate Change, Bor, Serbia.
- [15] Annual report on air quality in the Republic of Serbia in 2016, Republic of Serbia, Ministry of Environmental Protection, Environmental protection agency, Belgrade, Serbia. <https://sepa.gov.rs/wp-content/uploads/2024/10/Vazduh2016.pdf>. Accessed 2017.
- [16] Annual report on air quality in the Republic of Serbia in 2017, Republic of Serbia, Ministry of Environmental Protection, Environmental protection agency, Belgrade, Serbia. <https://sepa.gov.rs/wp-content/uploads/2024/10/Vazduh2017.pdf>. Accessed 2018.
- [17] Seechurn Y, Surnam B, Wharton J. Marine atmospheric corrosion of carbon steel in the tropical microclimate of Port Louis. *Mater Cor.* 2022; 73: 1474-1489. <https://doi.org/10.1002/maco.202112871>
- [18] Pan C, Han W, Wang Z, Wang C, Yu G. Evolution of Initial Atmospheric Corrosion of Carbon Steel in an Industrial Atmosphere. *JMEP.* 2016; 25: 5382-5390. <https://doi.org/10.1007/s11665-016-2312-0>
- [19] Wu H, Luo Y, Zhou G. The Evolution of the Corrosion Mechanism of Structural Steel Exposed to the Urban Industrial Atmosphere for Seven Years. *Appl Sci.* 2023; 13: 4500. <https://doi.org/10.3390/app13074500>
- [20] Qin H, Liu J, Shao Q, Zhang X, Teng Y, Chen S, Zhang D, Bao S. Corrosion behavior and cellular automata simulation of carbon steel in salt-spray environment. *Mater Degrad.* 2024; 8: 29. <https://doi.org/10.1038/s41529-024-00447-9>
- [21] De la Fuente D, Díaz I, Simancas J, Chico B, Morcillo M. Long-term atmospheric corrosion of mild steel. *Cor Sci.* 2011; 53: 604-617. <https://doi.org/10.1016/j.corsci.2010.10.007>
- [22] Dhaiveegan P, Elangovan N, Nishimura T, Rajendran N. Weathering Steel in Industrial-Marine-Urban Environment: Field Study. *MaterTrans.* 2016; 57, (2): 148-155. <https://doi.org/10.2320/matertrans.M2015345>
- [23] ISO Standard 9223:2012 Corrosion of metals and alloys — Corrosivity of atmospheres — Classification, determination and estimation. <https://www.iso.org/standard/53499.html>
- [24] ISO Standard 9226:2012 Corrosion of metals and alloys—Corrosivity of atmospheres—Determination of corrosion rate of standard specimens for the evaluation of corrosivity. <https://www.iso.org/standard/53502.html>
- [25] Montoya P, Díaz I, Granizo N, de la Fuente D, Morcillo M. An study on accelerated corrosion testing of weathering steel. *Mater. Chem. Phys.* 2013; 142: 220-228. <https://doi.org/10.1016/j.matchemphys.2013.07.009>
- [26] Zhang Z, Xu Y, Qin G, Xu S, Li R. Deterioration of Mechanical Properties and the Damage Constitutive Model of Corroded Steel in an Industrial Environment. *Materials.* 2022; 15: 8841. <https://doi.org/10.3390/ma15248841>

# Eksperimentalna analiza atmosferske korozije čelika S235JR u industrijskoj sredini

Jelena N. Stefanović<sup>1</sup>, Zoran Mišković<sup>2</sup>, Stevan Dimitrijević<sup>3</sup>, Zlatko Marković<sup>2</sup> i Milan Spremić<sup>2</sup>

<sup>1</sup>Institut za rudarstvo i metalurgiju Bor, Bor, Srbija

<sup>2</sup>Univerzitet u Beogradu, Građevinski fakultet, Beograd, Srbija

<sup>3</sup>Inovacioni centar Tehnološko-metalurškog fakulteta, Beograd, Srbija

(Naučni rad)

*Izvod*

U ovom radu ispitana je atmosferska korozija konstrukcionog čelika S235JR u industrijskoj sredini. Opšta ispitivanja korozije vršena su u blizini fabrike sumporne kiseline, u postrojenju za elektrolitičku rafinaciju i pored automatske stanice za praćenje kvaliteta vazduha u Boru u periodu od 6 meseci. Za ispitivanje međusobnog dejstva korozije i zagađenja industrijske sredine, korišćen je čelik S235JR, a njegove mehaničke karakteristike su dobijene ispitivanjem zatezanjem. Određeni su i meteorološki parametri, kao i zagađujuće materije u atmosferi (uglavnom SO<sub>2</sub>). Rendgenska difrakciona analiza (engl. X-ray diffraction, XRD) je korišćena za identifikaciju mineraloškog sastava produkata korozije. XRD analiza može ukazati na vezu između gubitka nosivosti i vrste sredine u kojoj se korozija razvija. Na osnovu dobijenih rezultata vrši se dalje predviđanje degradacije materijala usled korozije u industrijski agresivnoj sredini. Istraživanja u okviru ovog rada su omogućila bolje razumevanje ponašanja konstrukcionog čelika S235JR u kom je došlo do redukcije nosivosti usled korozije. Utvrđeno je da su produkti korozije različita jedinjenja u zavisnosti od sadržaja zagađujućih materija u atmosferi i lokacije čeličnih elemenata.

*Ključne reči:* Ispitivanje korozije; atmosferske korozione stanice; produkti korozije; SO<sub>2</sub>; XRD analiza; ispitivanje zatezanjem